MEMO: ANOMALIES IN GRAPHITE TSL.

FROM: JOSE IGNACIO MARQUEZ DAMIAN, DANILA ROUBTSOV

TO: CSEWG EXECUTIVE COMMITTEE

The proposed evaluations for coherent solids from NCSU cannot be fully reproduced from the LEAPR inputs available in the GForge server. This affected the ability to test the data, and to compute scattering cross sections at other temperatures.

In order to fix this, and based on the request of one user who needed Beryllium data at 77 K, we prepared a calculation scheme using the newly released code NCrystal [1], which is an open source tool to model the interaction of neutrons with crystalline materials. We call this calculation scheme NJOY-NCrystal [4]. We validated the tool against the ENDF/B-VIII.0β4 beryllium evaluation with satisfactory results (Fig. 1).

Then we moved on to graphite, and we found an anomalous behavior of the total cross section. Further investigation led to find a series of discrepancies, particularly in the case of the ”reactor graphite” model.

The findings are summarized below:

Anomalies in the total cross section

The total cross section for a solid moderator in the epithermal asymptotic range has a known theoretical behavior studied by Placzek [2]: the two components of the cross section (elastic and inelastic) should compensate each other and reach the free gas value. For a simple incoherent model, the way the total cross section reaches this value is described by (Fig. 2):

$$\sigma = \sigma_{\text{free}} \left[1 + \frac{C_1}{E} \left(1 - \frac{C_2}{E^2} \right) \right] \tag{1}$$

Although this is strictly valid only for incoherent moderators, it has been proved that the asymptotic expressions are also applicable to coherent moderators like graphite [3].

The total cross section calculated with the ENDF/B-VIII.0β4 models for graphite and reactor graphite show ”bumps” and ”valleys” in the asymptotic epithermal range ($0.1 - 1.0$ eV). Although we cannot say this with certainty without having access to the codes and models utilized by NCSU to evaluate the elastic component, we think that these anomalies are caused by an inconsistency between the evaluation of the inelastic and elastic components: the rise of the inelastic cross section is not compensated by the decrease of the the elastic cross section. This was particularly drastic in ENDF/B-VIII.0β4 reactor graphite, where the elastic component was simply copied and pasted from the graphite evaluation.

In the evaluations proposed for beta5 the anomaly in the total cross section of reactor graphite was partially reduced (Fig. 3), and the anomaly in crystalline graphite reversed in sign (Fig. 4). These changes have a significant effect in reactor calculations, as we show below.

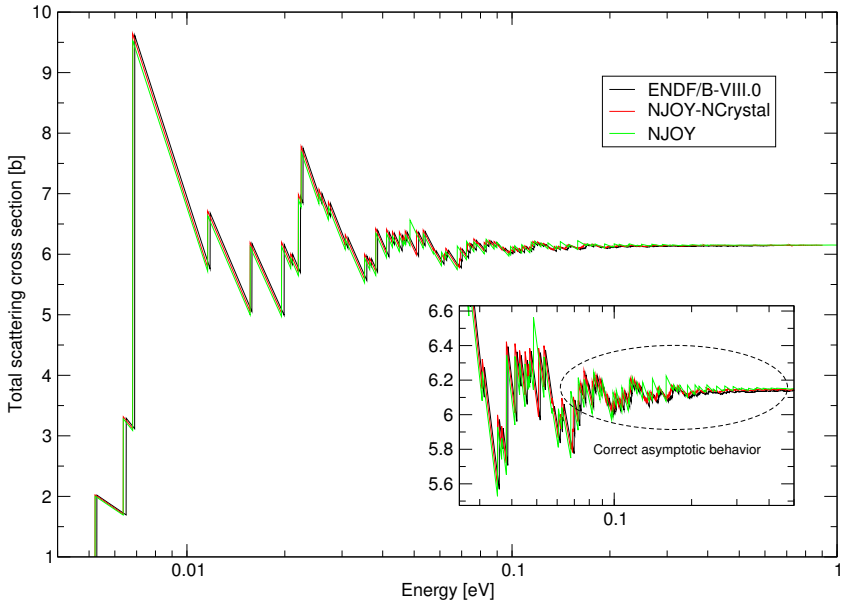

Figure 1: Total scattering cross section for beryllium metal.

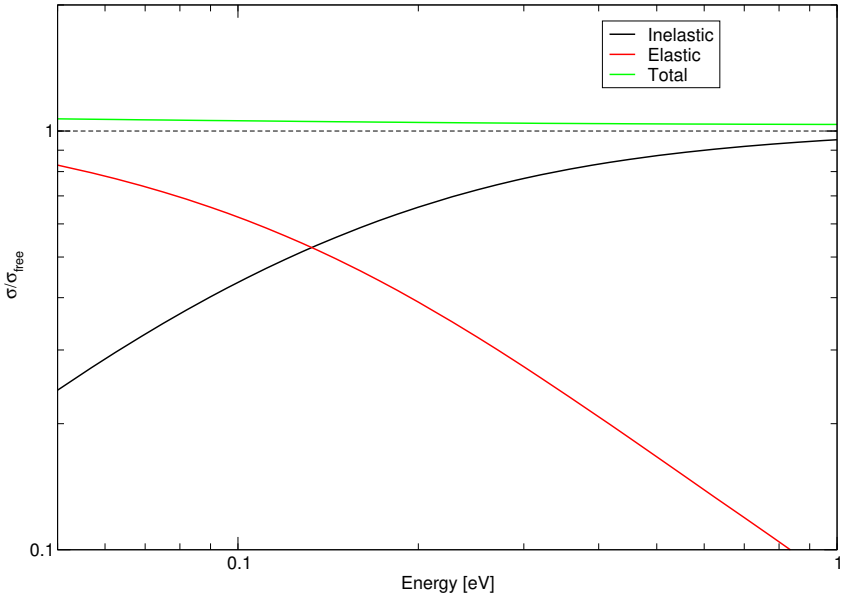

Figure 2: Typical total scattering cross section for an incoherent solid.

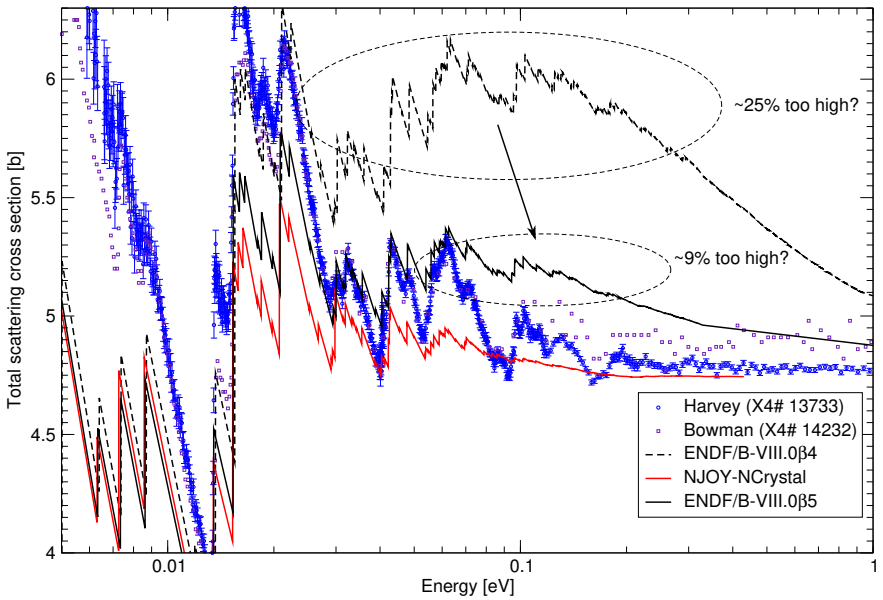

Figure 3: Total cross section for the reactor graphite model.

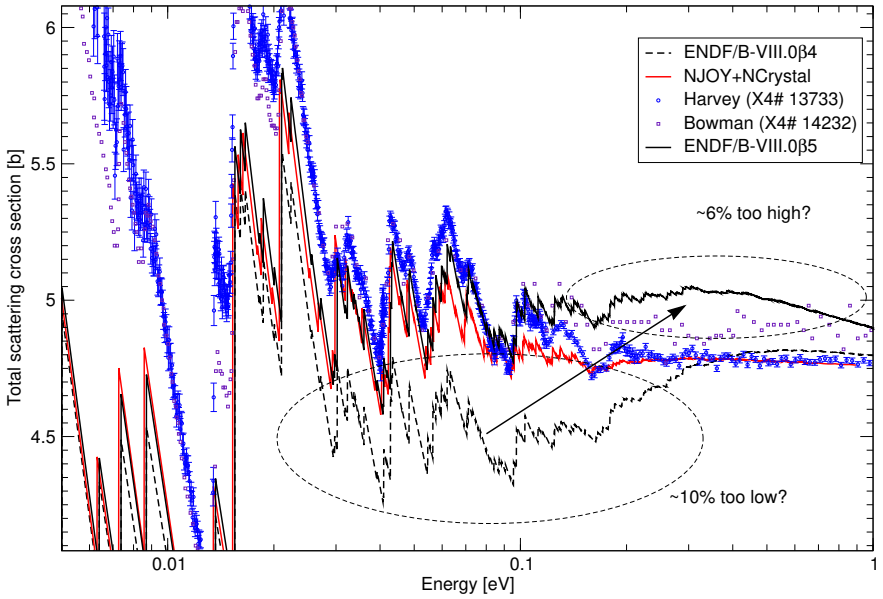

Figure 4: Total cross section for the cristalline graphite model.

Effects in criticality calculations

As noted by Steven Van der Marck, the calculation of graphite moderated reactors is significantly impacted by the use of the proposed ENDF/B-VIII.0 graphite TSL evaluations. We repeated the calculation of selected benchmark cases, using different combinations of data to ensure that the changes were caused by the TSL.

We started running benchmark HEU-COMP-THERM-016, case 4 ($k_{\text{bench}} = 1.00000 \pm 0.01100$) with the ENDF/B-VII ACE files shipped with MCNP5:

Case	k_{eff}	k_{eff} **change [pcm]**	$C/E-1$ **[pcm]**
Base ENDF/B-VII.0 calculation:	1.00864		864
Reactor graphite beta4:	1.04365	+3501	4365
Reactor graphite beta5:	1.02513	+1649	2513
NJOY-NCrystal:	1.01530	+666	1530
Graphite beta4:	1.00221	−643	221
Graphite beta5:	1.01440	+576	1440
NJOY-NCrystal:	1.01141	+277	1141
No S(a,b) (Free gas):	1.03477	+2613	3477

We repeated the calculation with ENDF/B-VIII.0β5 ACE files generated with ADVANCE:

Case	k_{eff}	k_{eff} **change [pcm]**	$C/E-1$ **[pcm]**
Base ENDF/B-VIII.0β5 calculation: (with ENDF/B-VII TSL)	1.00318		318
Reactor graphite beta4:	1.03747	+3429	3747
Reactor graphite beta5:	1.01937	+1619	1937
NJOY-NCrystal:	1.00976	+658	976
Graphite beta4:	0.99722	−596	−278
Graphite beta5:	1.00890	+572	890
NJOY-NCrystal:	1.00601	+283	601
No S(a,b) (Free gas):	1.02848	+2530	2848

And, to be sure, we also separated carbon in C-12 and C-13 to check the effect of the new libraries:

Case	$k_{\mathbf{eff}}$	$k_{\mathbf{eff}}$ **change [pcm]**	$C/E-1$ **[pcm]**
Base ENDF/B-VIII.0 calculation: (C-12/C-13 with ENDF/B-VII TSL)	1.00336		336
Reactor graphite beta4:	1.03797	+3461	3797
Reactor graphite beta5:	1.02099	+1763	2099
NJOY-NCrystal:	1.01142	+806	1142
Graphite beta4:	0.99901	−435	−99
Graphite beta5:	1.01046	+710	1046
NJOY-NCrystal:	1.00769	+433	769
No S(a,b) (Free gas):	1.02967	+2631	2967

Similar results were obtained for the IRPHE PROTEUS-GCR-EXP-001-CRIT, case 3 (k_{bench} = 1.00290 ± 0.00330):

Case	$k_{\mathbf{eff}}$	$k_{\mathbf{eff}}$ **change [pcm]**	$C/E-1$ **[pcm]**
Base ENDF/B-VII.0 calculation:	1.01123		833
Reactor graphite beta4:	1.03132	+2009	2842
Reactor graphite beta5:	1.02074	+951	1784
NJOY-NCrystal:	1.01436	+313	1146
Graphite beta4:	1.00610	−513	320
Graphite beta5:	1.01478	+355	1188
NJOY-NCrystal:	1.01129	+6	839
No S(a,b) (Free gas):	1.02756	+1633	2466

Case	$k_{\mathbf{eff}}$	$k_{\mathbf{eff}}$ **change [pcm]**	$C/E-1$ **[pcm]**
Base ENDF/B-VIII.0β5 calculation: (with ENDF/B-VII TSL)	0.99811		−479
Reactor graphite beta4:	1.01893	+2082	1603
Reactor graphite beta5:	1.00788	+977	498
NJOY-NCrystal:	1.00096	+285	−194
Graphite beta4:	0.99400	−411	−890
Graphite beta5:	1.00225	+414	−65
NJOY-NCrystal:	1.00000	+189	−290
No S(a,b) (Free gas):	1.01554	+1743	1264

As it can be seen from the results the changes in the elastic cross section are directly

related to the criticality of these systems: the models that overestimate the total cross section in the thermal-epithermal range (beta4 and beta5 reactor graphite, and beta5 graphite) show a positive change in the multiplication factor, whereas graphite beta4 (which underestimates the total cross section in the same region) shows a negative change in the multiplication factor. The results listed *NJOY-NCrystal* in the previous tables are the NCSU LEAPR inputs for graphite and reactor graphite computed with our code are examples of what would be expected if the elastic cross section is corrected, and overall show better agreement.

Thus, the bias is caused by the anomalies in the total cross section noted in the previous section, possibly because of changes in the diffusion coefficient in the transition between thermal and epithermal energies. In the case of reactor graphite, this effect is in some cases even larger than not using a TSL at all. The beta4 results are compatible to what was presented by NCSU at the ANS Winter Meeting 2017 [5] but, likely due to an unfortunate cancellation of errors, this $>$ 2000 pcm change was considered an improvement.

Despite the results are improved when the elastic cross section is corrected by using NJOY-NCrystal, there is still a large bias of 1000 - 1500 pcm in the calculations using the reactor graphite TSL. This motivated a more detailed analysis of this evaluation.

Additional inconsistencies of the reactor graphite evaluation

The reactor graphite evaluation attempts to explain the raise of the cross section of graphite below the lowest energy Bragg edge (Fig. 5) by using a frequency spectrum obtained in a molecular dynamics simulation of an imperfect arrangement of carbon atoms [6]. This imperfect arrangement introduces low energy modes to the frequency spectrum, which in turn increment the probability of low energy scattering. These changes should be measurable in the frequency spectrum by inelastic neutron scattering and could be checked in measurements of the specific heat capacity. Also, if this is the cause, the effect in the total cross section would be temperature dependent.

An alternative explanation, sustained by many authors [7, 8, 9](including, paradoxically, Ayman Hawari [10]) is that this increase of the total cross section at low energy is caused by elastic small angle neutron scattering caused by pores and cracks present in real (non crystalline) graphite. Under this explanation, the frequency spectrum should be similar to crystalline graphite, the specific heat capacity would not be affected, and the effect in the total cross section would be essentially temperature independent.

The first test we made was to check if the MD calculations by NCSU reproduce the frequency spectrum actually observed on reactor graphite. To do this we compared the calculations with experimental measurements by Hawari and Kolensnikov at SNS [11]. As it can be observed in Fig. 6, the MD simulation shows features not present in the measurements: the molecular dynamics result has a plateau in the 0-50 meV range, and the TO peak is shifted from $\sim$ 175 meV in the experiment to $\sim$ 209 meV in the MD result. The experimental results (although softened) actually show the same features observed in the frequency spectra of crystalline graphite.

The second test was to compute the specific heat capacity, using the different spectra:

$$C_v = 3R \int_0^\infty \mathrm{d}\omega\, \rho(\omega)\, [\beta\omega]^2\, \frac{e^{\beta\omega}}{\left(e^{\beta\omega} - 1\right)^2} \tag{2}$$

where R the gas constant, and $\beta = \hbar/(kT)$.

As it is shown in Fig. 7, the heat capacity for different types of graphite (Acheson graphite [12], natural Ceylon graphite [13] and industrial graphite [14]) are much better described by the frequency spectrum of crystalline graphite.

Finally, we studied the behavior of the total cross section with temperature, and compared the predictions of the NCSU model with the SANS model proposed by Petriw [8]. Palevsky [15] measured the total cross section of graphite below the lowest Bragg edge at different temperatures, and there is a discrepancy between what the current ENDF/B-VII model predicts and what is actually measured (Fig. 8). That difference, if it is caused by small angle neutron scattering, should be characterized only by the size and distributions of microscopic pores and cracks present in graphite, which is essentially temperature independent. On the other hand, if that difference is caused by inelastic effects (changes in the frequency spectrum), like the NCSU reactor graphite model assumes, it should increase with temperature.

As it can be seen in Fig. 9, the change in total cross section is essentially temperature independent, and roughly follows a λ^2 law, which is what we would expect if the change is caused by SANS. The black line in the plot is a fit of the SANS model proposed by Petriw:

$$\sigma_{\mathrm{SANS}}(\lambda) = \left(7.13736 \times 10^{-3}\,\mathrm{b\AA}^{-3}\right) \frac{P}{1-P} \lambda^2 r_p \left(1.09341 - \frac{0.005277\lambda^2}{r_p^2}\right) \tag{3}$$

with a pore volume fraction of $P = 2\,\%$ and a pore radius $r_p = 30\,\mathrm{\AA}$, which are reasonable values for graphite (Palevsky does not provide data on porosity in his paper).

We think this is the reason the reactor-graphite model overestimates the total cross section below the lowest Bragg edge for high temperatures (Fig. 10).

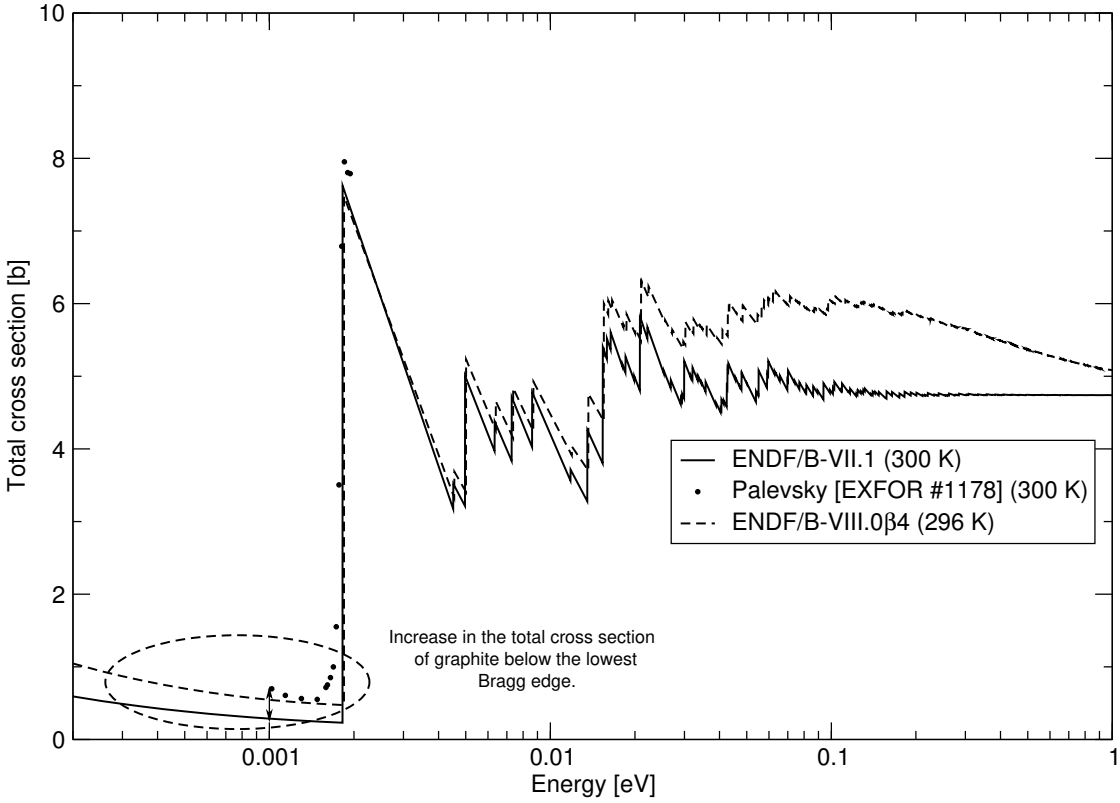

Figure 5: Total cross section for graphite measured by Palevsky compared with ENDF/B-VII and ENDF/B-VIII.0β4 (reactor graphite). The region that is highlighted is discussed in this section.

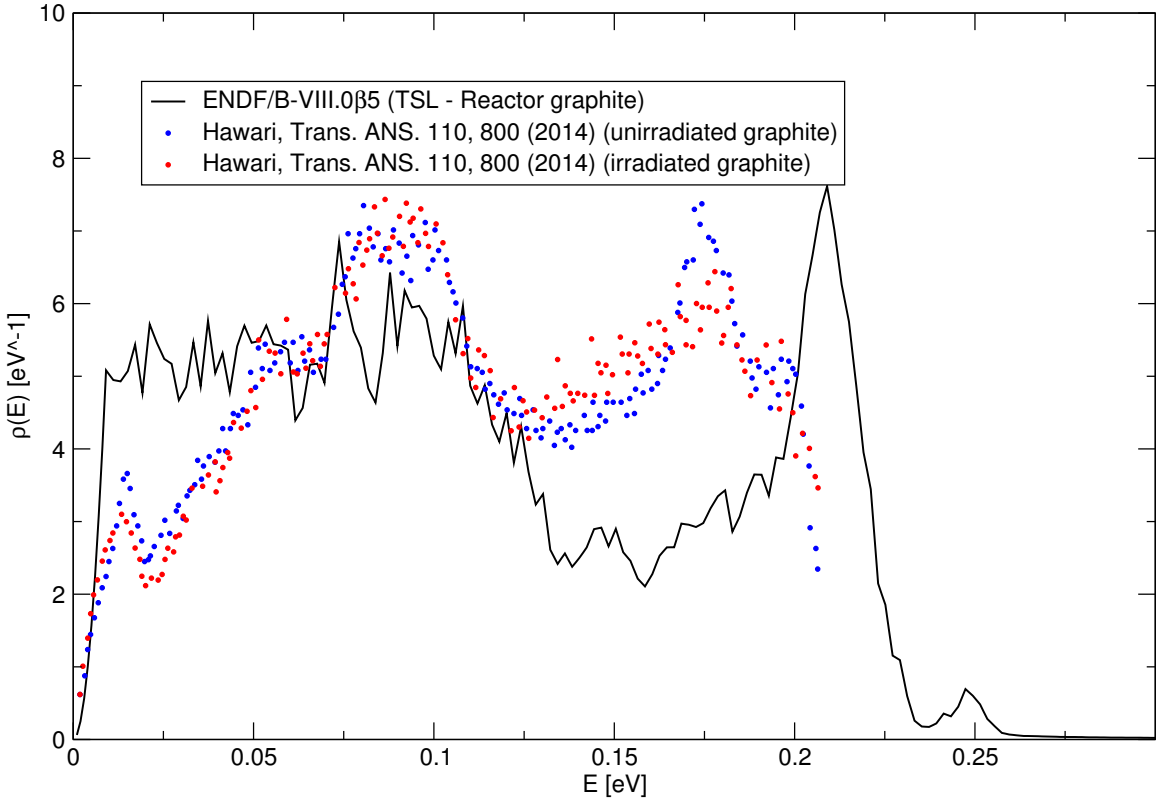

Figure 6: Experimental frequency spectra for reactor graphite with unirradiated (red) and irradiated (blue) samples, compared with the frequency spectrum used in the reactor graphite model.

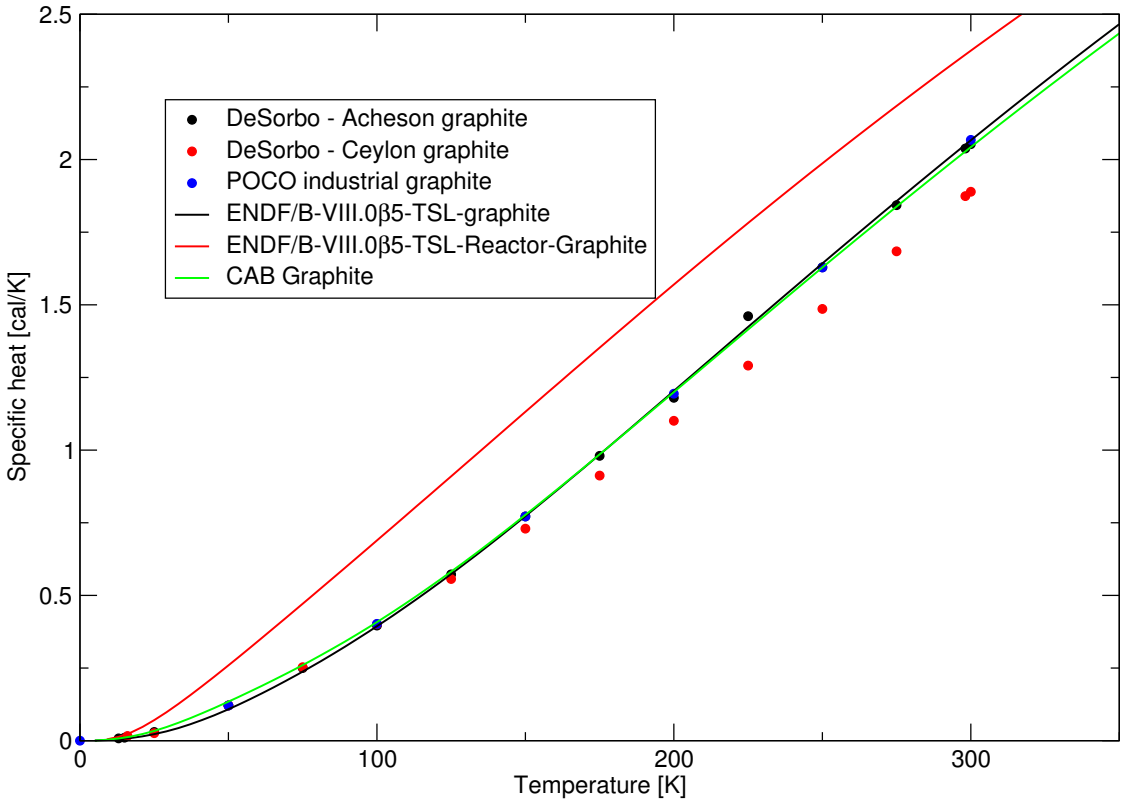

Figure 7: Specific heat capacity measured by DeSorbo on different types of graphite (Acheson graphite, and natural Ceylon graphite), and POCO graphite (industrial quality graphite), compared with calculations with different spectra.

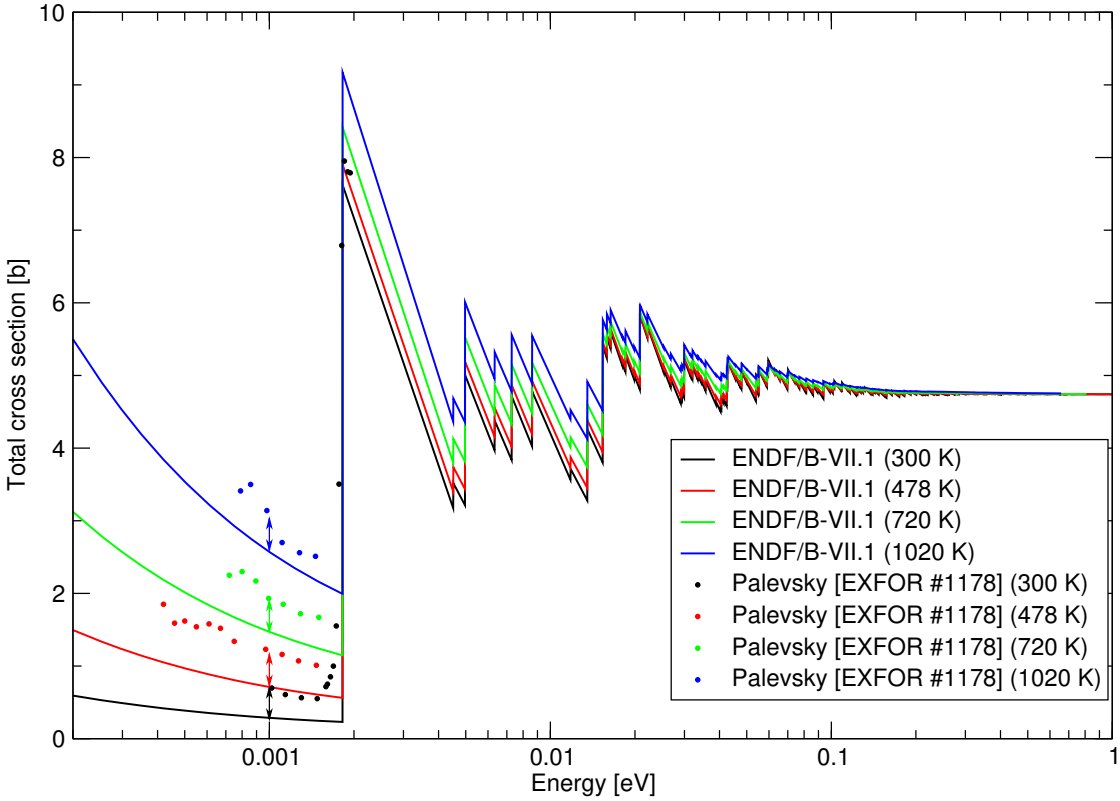

Figure 8: Experimental total cross section measured by Palevsky at different temperatures, compared with calculations with ENDF/B-VII. If the differences (marked with arrows) is what the inelastic (NCSU) or SANS models intend to correct.

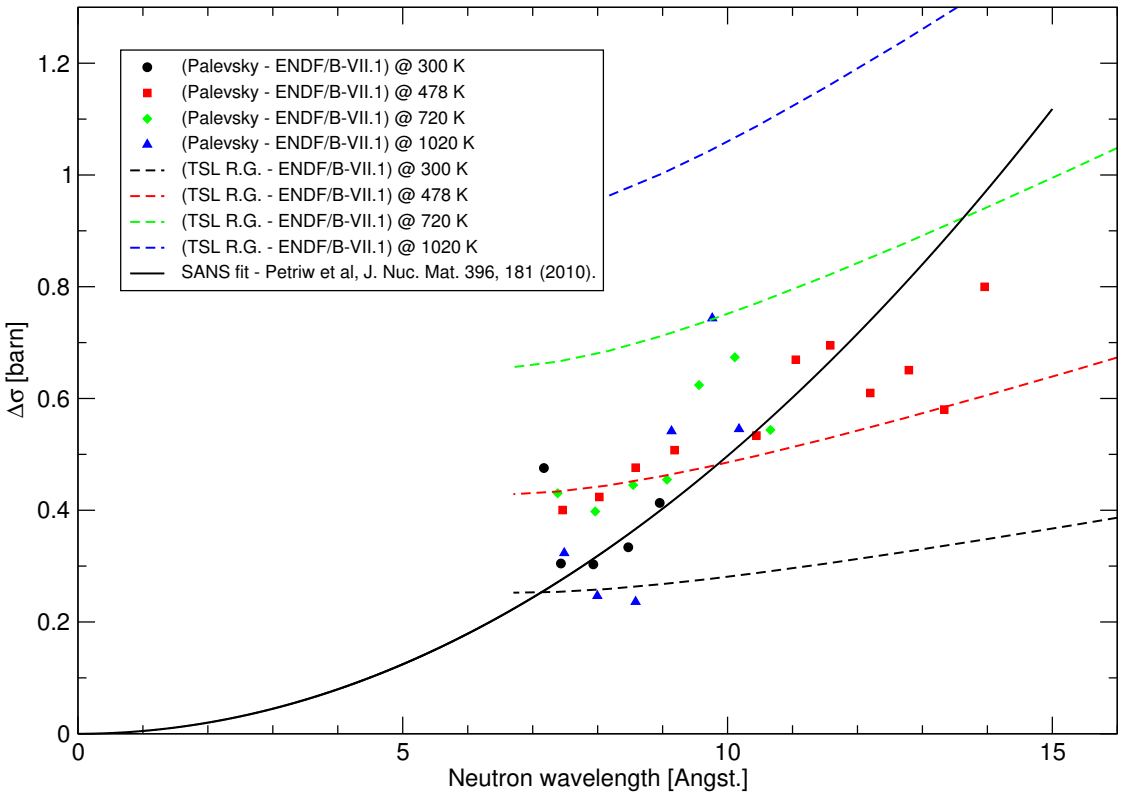

Figure 9: Differences in the total cross sections plotted in Fig. 8, compared with a temperature-independent model (SANS) and with an inelastic model (NCSU).

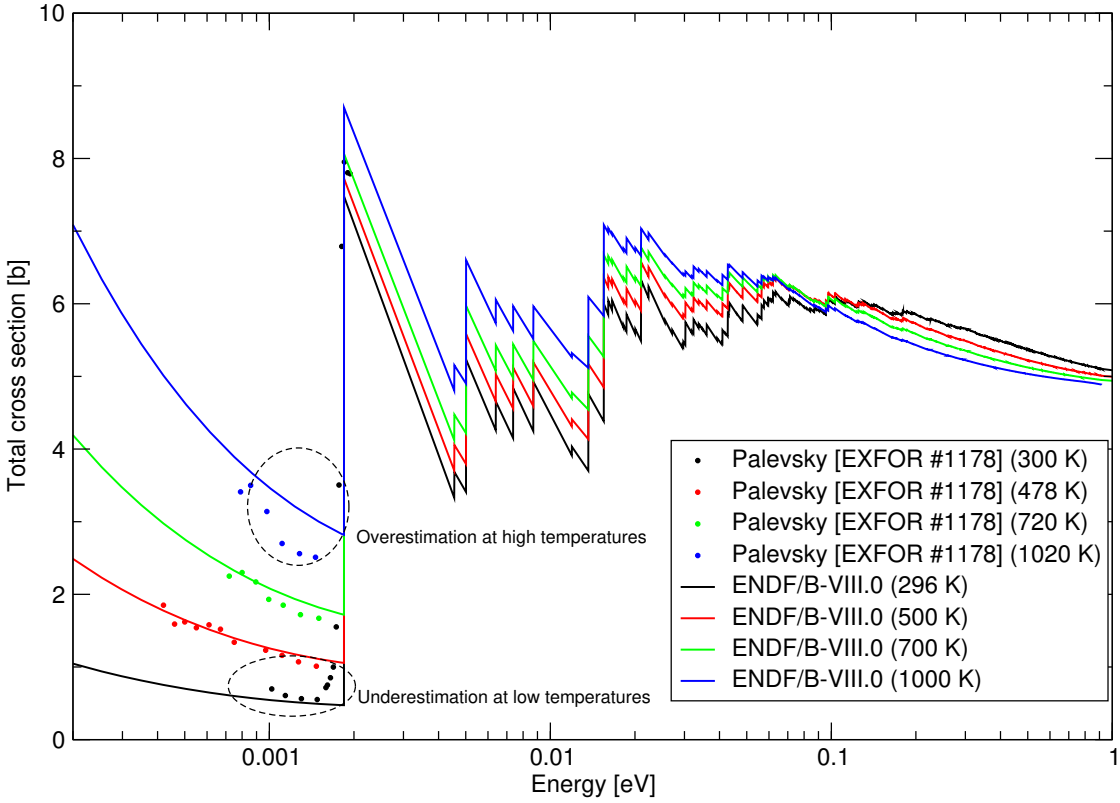

Figure 10: Experimental total cross section measured by Palevsky at different temperatures, compared with calculations with ENDF/B-VIII.0 reactor graphite. The model underestimates the total cross section at low temperatures, and overestimates the total cross section at high temperature, both in the beta4 and beta5 versions.

Conclusions

The models for graphite and reactor graphite in ENDF/B-VIII.0 show discrepancies that need further review. In the case of crystalline graphite, it would be necessary to review the elastic component to ensure that both the elastic and inelastic components are evaluated in a consistent way.

In the case of ”reactor graphite” there are a number of inconsistencies with experimental data, from the fundamental model to the derived quantities. The comparison shows that what this models seeks to fix, is better explained by the presence of small angle neutron scattering. A realistic model for graphite should include this effect and/or the presence of an amorphous carbon phase, and be validated against experimental data.

References

[1] X. X. Cai and T. Kittelmann. *NCrystal.* `https://doi.org/10.5281/zenodo.853186`

[2] G. Placzek. *The scattering of neutrons by systems of heavy nuclei*. Physical Review. **86**, 377 (1952).

[3] J.R. Granada. *Total scattering cross section of solids for cold and epithermal neutrons*. Zeitschrift für Naturforschung. **39**, 1160 (1984).

[4] J.I. Marquez Damian. *NJOY-NCrystal Tutorial.* `https://gist.github.com/marquezj/625407e8ff60fb4b41f1bf8f8db6a6c3`

[5] N.C. Sorrell, et al. *Investigation of Treat M2 and M3 Calibration Experiments for Benchmark Analysis*. ANS Transactions. **116**, 1225 (2017).

[6] A.I. Hawari and V. H. Gillete. *Inelastic thermal neutron scattering cross sections for reactor-grade graphite*. Nuclear Data Sheets. **118**, 176 (2014).

[7] A. Steyerl, and W-D. Trustedt. *Experiments with a neutron bottle*. Zeitschrift für Physik A Hadrons and Nuclei. **267**, 379 (1974).

[8] S. Petriw, J. Dawidowski, and J. Santisteban. *Porosity effects on the neutron total cross section of graphite*. Journal of Nuclear Materials. **396**, 181 (2010).

[9] VM Galvan Josa, et al. *Model for neutron total cross-section at low energies for nuclear grade graphite*. Nuclear Instruments and Methods A. **780**, 27 (2015).

[10] C.R. Gould, A. I. Hawari, and E. I. Sharapov. *Re-Analysis of Recent Neutron Diffusion and Transmission Measurements in Nuclear Graphite*. Nuclear Science and Engineering. **165**, 200 (2010).

[11] A.I. Hawari, et al. *Inelastic Neutron Scattering Analysis of Reactor Grade Graphite*. Embedded Topical Meeting on Nuclear Fuels and Structural Materials for the Next Generation Nuclear Reactors, Reno, NV, 2014.

[12] W. DeSorbo and W. W. Tyler. *The specific heat of graphite from 13 to 300 K*. The Journal of Chemical Physics. **21**, 1660 (1953).

[13] W. DeSorbo. *Low temperature heat capacity of Ceylon graphite*. Journal of the American Chemical Society. **77**, 4713 (1955).

[14] POCO Graphite, Inc. *Properties and Characteristics of Graphite*. (2015).

[15] H.Palevsky, D.J.Hughes, R.L.Zimmerman. *Inelastic Scattering of Cold Neutrons by the Lattice Vibration of Crystalline Solids*. Physical Review. **99**, 611 (1955).